# Syndecan regulates cell migration and axon guidance in *C. elegans*

**Christa Rhiner[1,2], Stephan Gysi[1], Erika Fröhli[3], Michael O. Hengartner[1,2,*] and Alex Hajnal[3]**

[1]Institute of Molecular Biology, University of Zurich, 8057, Switzerland
[2]Neuroscience Center, 8057, Zurich, Switzerland
[3]Institute of Zoology, University of Zurich, 8057, Switzerland
*Author for correspondence (e-mail: michael.hengartner@molbio.unizh.ch)

*Accepted 17 August 2005*

Development 132, 4621-4633
Published by The Company of Biologists 2005
doi:10.1242/dev.02042

## Summary

**During nervous system development, axons that grow out simultaneously in the same extracellular environment are often sorted to different target destinations. As there is only a restricted set of guidance cues known, regulatory mechanisms are likely to play a crucial role in controlling cell migration and axonal pathfinding. Heparan sulfate proteoglycans (HSPGs) carry long chains of differentially modified sugar residues that have been proposed to encode specific information for nervous system development. Here, we show that the cell surface proteoglycan syndecan SDN-1 functions autonomously in neurons to control the neural migration and guidance choices of outgrowing axons. Epistasis analysis suggests that heparan sulfate (HS) attached to SDN-1 can regulate guidance signaling by the Slit/Robo pathway. Furthermore, SDN-1 acts in parallel with other HSPG core proteins whose HS side chains are modified by the C5-epimerase HSE-5, and/or the 2*O*-sulfotransferase HST-2, depending on the cellular context. Taken together, our experiments show that distinct HS modification patterns on SDN-1 are involved in regulating axon guidance and cell migration in *C. elegans*.**

Key words: Axon guidance, *C. elegans*, Cell migration, Heparan sulfate proteoglycan, Syndecan

## Introduction

During nervous system development, migrating cells and axonal growth cones are guided by extracellular stimuli to their final position in the body. Although several major families of attractive and repulsive guidance cues have been characterized, it is not clear how the presence of multiple directional cues are integrated by a single outgrowing axon while leaving other neurons unaffected. Recent findings indicate that heparan sulfate proteoglycans (HSPGs) act as crucial modulators of axon guidance choices (Lee and Chien, 2004). HSPGs are present both on the cell surface and in the extracellular matrix, where they modulate cellular responses to extracellular signals in various developmental and pathological processes (Sasisekharan et al., 2002; Topczewski et al., 2001). Their function in nervous system development has long been presumed, but only recent genetic studies have provided in vivo evidence for their role in axon pathfinding (Bülow and Hobert, 2004; Inatani et al., 2003; Johnson et al., 2004; Lee et al., 2004; Steigemann et al., 2004).

HSPGs consist of a secreted or membrane-anchored protein core to which several heparan sulfate (HS) polysaccharide chains are attached (Bernfield et al., 1999; Esko and Selleck, 2002; Lindahl et al., 1998). Once the HS chain is synthesized, specific enzymes – including sulfotransferases and an epimerase – modify the individual sugar moieties, resulting in complex modification patterns (Lindahl et al., 1998). A complete lack of HS abrogates multiple signaling pathways essential for early development, resulting in severe patterning defects and lethality (Inatani et al., 2003; Bornemann et al., 2004; Herman et al., 1999; Morio et al., 2003; Perrimon and Bernfield, 2000). Together with the biochemical studies, these observations led to the hypothesis that HSPGs act as co-receptors that bind and sequester extracellular signals in the extracellular matrix (Bernfield et al., 1999; Perrimon and Bernfield, 2000).

By contrast, genetic removal of enzymes that secondarily modify HS, including sulfotransferases and an epimerase, demonstrated that specific modifications are needed for distinct axon guidance choices (Bülow and Hobert, 2004). Hence, it has been proposed that individual HS modifications in a given area or on specific neurons give rise to a 'sugar code' that regulates axon guidance by modulating specific receptor-ligand interactions. So far it is not known, however, which core proteins are crucial in this process and how they function to modulate axon guidance signaling. Syndecans and glypicans are the two major families of cell surface-bound HSPGs (Fig. 1A). In mice, the inactivation of a single syndecan gene does not result in any obvious phenotype, probably due to redundancy between the family members (Hartmann and Maurer, 2001; Bernfield et al., 1999).

Syndecan mutant flies display a Robo-like midline phenotype, which can be rescued by overexpression of either syndecan or the two *Drosophila* glypican genes *dally* and *dally-like* (Johnson et al., 2004; Steigemann et al., 2004). Furthermore, it was found that lack of syndecan affects the distribution of the midline repellent Slit, which provides the first indication of how HSPGs might function (Johnson et al., 2004).

Unlike mammals, which have four syndecan family members, the *Caenorhabditis elegans* genome contains one

single syndecan (*sdn-1*) gene. We show here that *C. elegans* syndecan SDN-1 functions autonomously in neurons to ensure correct cell migration and axon guidance. Epistasis analysis indicates that *sdn-1* participates in the Slit/Robo signaling pathway, which acts in parallel with a second, currently unknown, guidance system that relies on a different combination of sugar modifications on a distinct HSPG core protein. We therefore propose that at least two distinct HSPG members bearing cell-specific HS modification patterns are involved in regulating axon pathfinding and cell migration.

## Materials and methods

### *C. elegans* genetics

Standard methods were used for maintaining and manipulating *Caenorhabditis elegans* (Brenner, 1974). The *C. elegans Bristol* strain N2 was used as wild-type reference in all experiments. Animals were raised at 20°C unless indicated otherwise. The following mutations were used: LG III: *hse-5(tm472)* (Bülow and Hobert, 2004); LGX: *sdn-1(zh20)* (this study), *sdn-1(ok449)* (Minniti et al., 2004), *hst-6(ok273)* and *hst-2(ok595)* (Bülow and Hobert, 2004), *sax-3(ky123)* (Zallen et al., 1998), *slt-1(eh15)* (Hao et al., 2001). All transgenes used to score neuroanatomy were described previously (Bülow and Hobert, 2004; Bülow et al., 2002).

### Constructs

The $P_{sdn\text{-}1}$*::sdn-1::gfp* translational fusion construct pAH40 was generated by ligating a 5.7 kb *Bam*HI-*Sph*I fragment covering 2.8 kb of 5′ regulatory sequences and the entire coding region into the pPD95.75 vector (gift of A. Fire, Stanford University), such that the full-length *sdn-1* open reading frame was fused in frame to *gfp*. pAH40 and the *lin-15* rescuing plasmid pL15EK (gift of R. Horvitz) were co-injected (100 ng/μl of each) into *lin-15(n765ts)* animals to obtain transgenic lines. Two independent lines (*opIs170*, *opIs171*) showed similar expression patterns.

$P_{sdn\text{-}1}$*::sdn-1* (pAH46) was made by cloning a 6.9 kb genomic PCR product containing 2.8 kb of 5′ sequences, the entire *sdn-1* coding region and the predicted 3′UTR into the pGEM-T vector. The $P_{dpy\text{-}7}$*::sdn-1*(cDNA) construct was generated by fusion PCR (Hobert, 2002): the hypodermal promoter of *dpy-7* (216 bp) (Gilleard et al., 1997) was fused to the ATG start codon of the *sdn-1* cDNA. The $P_{sra\text{-}6}$*::sdn-1* plasmid (pCR1) and the $P_{unc\text{-}119}$*::sdn-1* plasmid (pCR2) were made by subcloning the *sra-6* promoter (3747 bp) or the *unc-119* promoter (2189 bp) sequence into pPD95.86 (gift of A. Fire, Stanford University), in front of the ATG start codon of the *sdn-1* cDNA. For rescue, worms were injected with 20 ng/μl of pAH46, pCR1 or pCR2, or with 2.5 ng/μl of the fusion construct $P_{dpy\text{-}7}$*::sdn-1*. Constructs were injected together with pTJ1157 (*lin-48::gfp*) and pBluescript SK at 50 ng/μl each, or, for the rescue of HSN migration, with pPD118.33 (*myo-2::gfp*) at 2.5 ng/μl.

### Isolation of the *sdn-1* deletion allele

The *sdn-1(zh20)* deletion mutant was isolated from an EMS-mutagenized library consisting of approximately $10^6$ haploid genomes, as previously described (Jansen et al., 1997; Berset et al., 2001). DNA pools were screened by nested PCR with the outer primers OAH40 (5′-TGGGTTCATCCAATGCGTATGACC-3′) and OAH49 (5′-CCCTATTCTGTCATTGTACCAC-3′), and the nested primers OAH41 (5′-TTGCCGTACACCGCCATTTCCTC-3′) and OAH48 (5′-AGAATGGCTGTAATCACCGCAACG-3′). The *zh20* deletion removes 1260 bp within the coding region (Fig. 1B). The sequence of the break point is as follows: TTTGCTTCACAC//zh20//GTCGACAGGCAG. The mutant strain was backcrossed six times to N2 before analysis.

### Phenotypic analysis

All mutant alleles were backcrossed at least four times before phenotypic analysis. Axon guidance defects were scored in staged young adults or L1 larvae using a Leica DMR microscope. Migration of HSN, ALM and CAN neurons and coelomocytes were scored in adult stages (HSN, ALM, CAN) and L3-L4 stages (coelomocytes).

### Statistical analysis

All phenotypes, except defects in guidance and left/right choices of D-type motoneurons (Fig. 6A), were scored as the percentage of animals that were defective, and are shown with error bars denoting the standard error of proportion. Statistical significance was calculated using the z-test. For the defects in D-type motoneurons, error bars give the standard error of the mean and statistical significance was calculated by using Student's *t*-test. If multiple comparisons were made, Bonferroni's correction was applied.

## Results

### Isolation of a *sdn-1* null allele

The *C. elegans* genome is predicted to code for only two cell surface-bound HSPGs genes, syndecan SDN-1 and glypican GPN-1 (Fig. 1A), and three extracellular HSPGs, agrin (F41G3.8) (Hutter et al., 2000), perlecan UNC-52 (Rogalski et al., 1993) and CLE-1, a homolog of collagen XVIII (Ackley et al., 2001; Halfter et al., 1998).

To study the role of SDN-1 in nervous system development, we first isolated a null allele of *sdn-1*. The deletion allele *sdn-1(zh20)* removes most of the *sdn-1* open reading frame (Fig. 1B). Furthermore, no *sdn-1* transcripts were detected on northern blots of RNA isolated from *zh20* animals (Fig. 1C). Thus, the *sdn-1(zh20)* allele most likely causes a complete loss of SDN-1 function. Homozygous *sdn-1(zh20)* animals are viable, but they show defects in backward locomotion, are variably egg-laying defective and have a slightly reduced brood size (201±42, $n$=10) when compared with wild-type worms (280±10, $n$=10).

A recent study carried out with a hypomorphic allele of *sdn-1* reported a role of SDN-1 in vulva development, but did not analyze neuronal phenotypes (Minniti et al., 2004). This published allele, *sdn-1(ok449)*, results in an in-frame deletion and produces a truncated form of SDN-1 lacking the two major conserved HS attachment sites in the extracellular domain (Fig. 1B). The truncated SDN-1 core protein in *ok449* animals could still be detected on western blots by using an antibody directed against the cytosolic tail, but was no longer recognized by a monoclonal antibody specific for HS side chains, indicating that there is considerably less, if any, HS attached to SDN-1 in this mutant (Minniti et al., 2004). We examined the neural phenotypes of both *sdn-1* mutants, but focused our epistasis analysis on the null allele *sdn-1(zh20)*, because the *ok449* deletion may not completely eliminate *sdn-1* function (Table 1).

### SDN-1 is necessary for the migration of different cell types

The formation of a functional nervous system starts with the migration of neural cell bodies to their genetically determined position. Thereafter, neurons extend axons that navigate to the target area to finally form synaptic contacts. The migrating neurons and axonal growth cones are guided by similar molecules. For example, UNC-6 Netrin controls both cell and

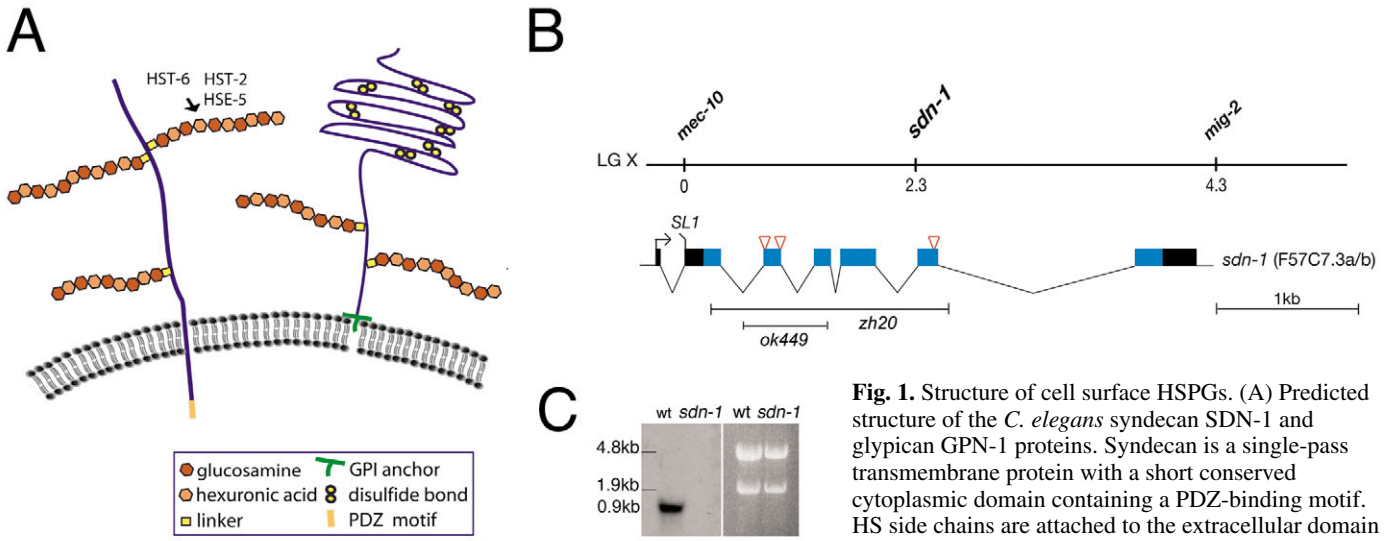


**Fig. 1.** Structure of cell surface HSPGs. (A) Predicted structure of the *C. elegans* syndecan SDN-1 and glypican GPN-1 proteins. Syndecan is a single-pass transmembrane protein with a short conserved cytoplasmic domain containing a PDZ-binding motif. HS side chains are attached to the extracellular domain of the core protein at conserved serine residues. The yellow box represents a typical tetrasaccharide linker region, which connects the HS chain to the serine. Glypican is attached to the cell surface by a GPI anchor. (B) Genomic structure of the *sdn-1* locus on chromosome X. Boxes represent exons (blue, coding; black, non-coding) and red triangles indicate putative HS attachment sites. Two isoforms of the *sdn-1* mRNA have been predicted to code for identical proteins. The null allele *sdn-1(zh20)* affects exons 1-5. The allele *ok449* was previously shown to produce a truncated syndecan form lacking the two major HS attachment sites (Minniti et al., 2004). (C) Northern blot analysis of *sdn-1*. A single message of approximately 0.9 kb is detected in wild-type worms, whereas no message can be found in *sdn-1(zh20)* mutants. 18S and 28S ribosomal RNAs, as loading controls, are shown to the right.

**Table 1. Summary of phenotypes in *sdn-1* mutants**

| Neurons examined (marker used) | % Animals defective | |
|---|---|---|
| | *sdn-1(zh20)* | Wild type |
| **A. Axon guidance** | | |
| Head neurons | | |
| Sensory neurons | | |
| AFD sensory neurons (*oyIs17*) | 0 | 0 |
| Amphid neurons (DiI) | 0 | 0 |
| Ventral cord neurons | | |
| Sensory neurons | | |
| AVM/PVM neurons (*zdIs5*) | | |
| – ventral axon guidance | 9±1 | 1±1 |
| Interneurons | | |
| PVT interneuron (*otIs39*) | 0 | 0 |
| AVK interneurons (*bwIs2*) | 36±2 | 4±1 |
| PVP interneurons (*hdIs26*) | 32±3 | 5±1 |
| PVQ interneurons (*oyIs14*) | 49±2 | 8±1 |
| Command interneurons (*rhIs4*) | 0 | 0 |
| Motoneurons | | |
| HSN motoneurons (*mgIs71*) – axon guidance* | 83±4* | 9±3 |
| D-type motoneurons (*oxIs12*) | | |
| – fasciculation VNC | 37±3 | 7±1 |
| – midline L/R choice† | 2.3† | 0.3† |
| – circumferential growth | 66±3 | 0 |
| – fasciculation DNC | 15±7 | 0 |
| DA/DB motoneurons (*evIs82b*) | | |
| – midline L/R choice† | 1.1† | 0† |
| Tail neurons | | |
| Sensory neurons | | |
| Phasmid neurons (DiI) | 0 | 0 |
| **B. Cell migrations** | | |
| HSN motoneurons (*mgIs71*) | 56±3 | 0 |
| CAN neurons (*otIs33*) | 39±2 | 6±2 |
| ALM sensory neurons (*zdIs5*) | 47±4 | 1±1 |
| Anterior coelomocytes (*otIs121*) | 69±2 | 3±1 |

*Part of the defects are caused by mispositioned HSN cell bodies.
†Number of commissures that exit the VNC on the inappropriate side/adult.

growth cone migrations along the dorsoventral axis (Chan et al., 1996; Hedgecock et al., 1987). To study the role of SDN-1 in different phases of nervous system development, we crossed *sdn-1* alleles into different reporter strains, in which specific types of neurons are labeled with *gfp* (Table 1). We observed no obvious changes in the overall organization of the nervous system in the major ganglia and nerve bundles in both *sdn-1* alleles when using a pan-neuronal *gfp* marker (data not shown).

When examining single neuron subtypes, however, we observed prominent migration defects of neural cell bodies. The HSN left (L)/right (R) motoneurons normally migrate during embryonic development from the posterior to the mid-body region (Fig. 2A). In both *sdn-1* alleles, the HSN neurons either failed to migrate at all or stopped prematurely before reaching their normal position near the vulva (Fig. 2C,D). A null mutation in the 2*O*-sulfotransferase *hst-2* gene causes similar HSN migration defects, although they are less severe than those observed in *sdn-1(zh20)* animals (Fig. 2E) (Bülow and Hobert, 2004; Kinnunen et al., 2005). By contrast, neither the 6*O*-sulfotransferase HST-6 nor the C5-epimerase HSE-5 is required for HSN migration (Bülow and Hobert, 2004), pointing to a crucial role of 2*O*-sulfated HS in this process. Double-null mutants of *sdn-1* and *hst-2* show significantly more HSN migration defects, indicating that 2*O*-sulfation, although possibly important for SDN-1 function, is also required for, at least, one additional HSPG (Fig. 2E). Loss of HSE-5 similarly enhances the HSN migration defects of *sdn-1* null mutants, whereas removal of HST-6 in a *sdn-1* background shows no increase of migration errors (Fig. 2E). Next, we tested posterior migration of the ALML/R sensory neurons. In the absence of SDN-1, ALML/R neurons stopped prematurely (Table 1). Migration defects of the ALML/R neurons have also been described in mutants for the *C. elegans*

Robo receptor SAX-3 (Zallen et al., 1999). We examined ALM migration errors of both *sdn-1(zh20)* and *sax-3(ky123)* mutants and found comparable defects [47% for *sdn-1(zh20)*, 45% for *sax-3(ky123)*]. In addition, loss of SDN-1 function impaired the posterior migration of the CANL/R neural cell bodies (Table 1).

Finally, we detected a cell migration defect of the macrophage-like coelomocytes, a non-neural cell-type. In wild-type hermaphrodites, four coelomocytes are born and migrate posteriorly during embryogenesis, whereas the two coelomocytes generated in the L1 stage do not migrate (Fig. 2F). In *sdn-1(zh20)* null mutants, the embryonic coelomocytes were often located too far anteriorly, just behind the pharynx (Fig. 2H). In all the cell migration events examined, SDN-1 always appeared to confer a pro-migratory property, irrespective of the direction of cell migration.

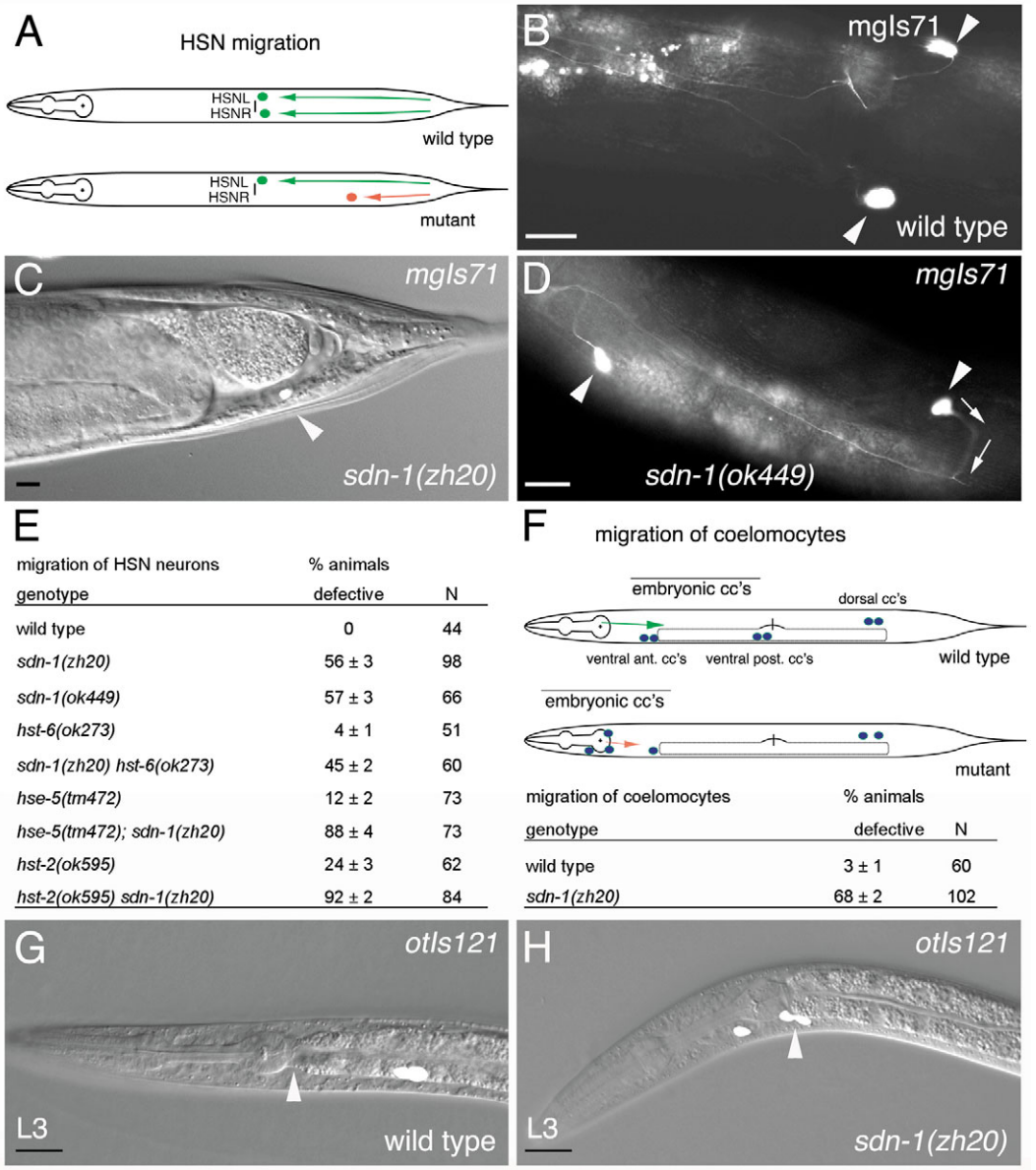


**Fig. 2.** SDN-1 is required for the migration of neurons and coelomocytes. (A) Schematic depicting the migration of HSN neurons during embryogenesis. (B) In wild-type animals both HSN cell bodies (arrowheads) locate close to the vulva. (C,D) In *sdn-1* mutants, HSN neurons fail to migrate to the vulva from their original position in the tail (C) or stall prematurely anterior to the vulva (D). Axons of mispositioned HSN bodies (arrowheads) that initially grow out incorrectly in a posterior direction eventually turn (arrows) and reach the nerve ring in the head. (E) HSN migration (adult stages) demonstrated by the genetic interaction of *sdn-1* nulls with HS-modifying enzyme mutants. '% animal defective' represents the fraction of animals with at least one defective HSN neuron. Numbers are shown with the standard error of proportion. (F) Schematic of the six coelomocytes in wild-type and *sdn-1(zh20)* hermaphrodites. (G) In the wild type, coelomocytes born in the head migrate caudally during embryonic development, past the intestinal valve that separates the pharynx from the intestine (arrowhead). (H) In *sdn-1* null mutants, coelomocytes are found in the head region, anterior and posterior of the intestinal valve (arrowhead). In order to define anatomical locations, some pictures were taken with DIC optics in the fluorescent channel (C,G,H). N, number of animals scored. Scale bars: 10 μm.

## SDN-1 is required for correct axon guidance at the midline

### Midline interneurons

Because mutants for the HS-modifying enzymes have previously been reported to display guidance defects of midline interneurons (Bülow and Hobert, 2004), we tested whether *sdn-1(zh20)* null mutants would show similar defects. The ventral nerve cord (VNC) runs along the left and right side of the ventral hypodermal ridge in two separate fascicles. We first examined the guidance of the PVQ interneurons, a pair of bilaterally symmetric neurons located in the tail (Fig. 3A). The PVQL and PVQR axons normally grow out to the head on the left and right side of the midline, respectively, without crossing to the contralateral side (Fig. 3A,B). In both *sdn-1* mutants, PVQ axons inappropriately crossed to the contralateral side or were entirely fused in a single track (Fig. 3C). Most crossover defects (75%) consisted of single or multiple midline crossings of PVQ axons along the entire length of PVQ extention, the remaining 25% showed entirely collapsed PVQ axons. The PVPL/R and AVK interneurons showed comparable crossover defects (Fig. 3F, Table 1).

### HSN motoneurons

In contrast to most axons, which join the VNC in the head or the tail, the axons of the HSN neurons join the VNC midway near the vulva and grow anteriorly without crossing the midline (Fig. 3G,H). In *sdn-1(zh20)* animals, HSN axons frequently crossed the midline

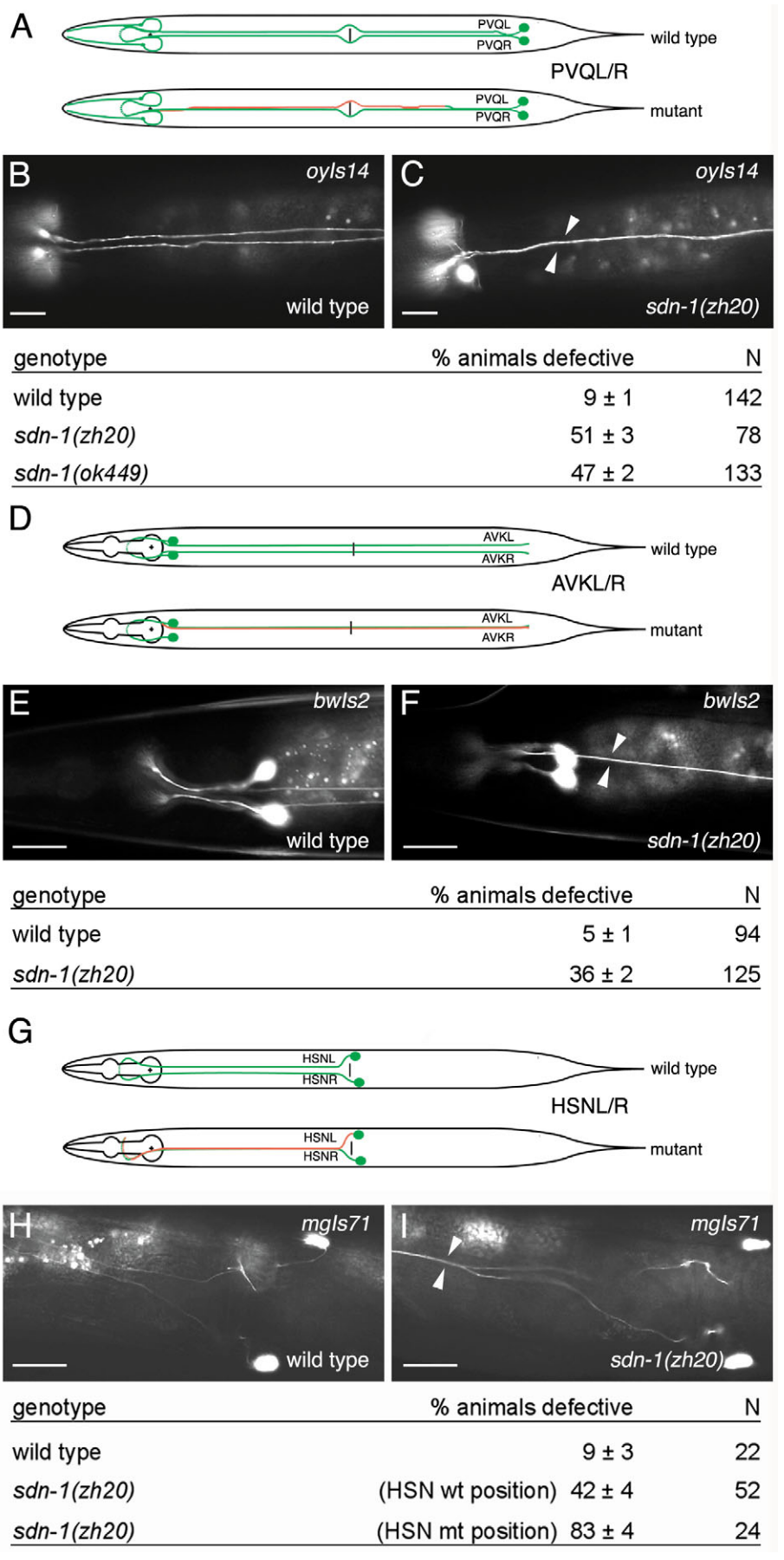


| genotype | % animals defective | N |
|---|---|---|
| wild type | 9 ± 1 | 142 |
| *sdn-1(zh20)* | 51 ± 3 | 78 |
| *sdn-1(ok449)* | 47 ± 2 | 133 |

| genotype | % animals defective | N |
|---|---|---|
| wild type | 5 ± 1 | 94 |
| *sdn-1(zh20)* | 36 ± 2 | 125 |

| genotype | % animals defective | N |
|---|---|---|
| wild type | 9 ± 3 | 22 |
| *sdn-1(zh20)* | (HSN wt position) 42 ± 4 | 52 |
| *sdn-1(zh20)* | (HSN mt position) 83 ± 4 | 24 |

**Fig. 3.** *sdn-1* mutants show midline crossover defects of VNC interneurons. (A) Schematic of PVQL/R interneurons. (B) PVQL/R interneurons run parallel to the head in the wild type. (C) PVQ axons inappropriately cross the midline in *sdn-1* mutants, leading to collapsed axon tracks (arrowheads). (D) Schematic of the AVKL/R interneurons. (E) Wild-type AVKL/R run next to each other, whereas midline crossing of AVKL/R axons can be observed in *sdn-1(zh20)* worms (arrowheads) (F). (G) Schematic of HSNL/R motoneurons. (H) HSNL/R stay ipsilateral in the wild type, whereas HSNL/R axons frequently cross to the contralateral side in *sdn-1(zh20)* null mutants (arrowheads) (I). All schematics and photos are ventral views, anterior is to the left. N, number of animals scored. Scale bars: 10 μm.

(Fig. 3I). As mentioned before, the HSN neurons frequently fail to migrate to their normal position in *sdn-1* mutants (Table 1). To determine whether the misplacement of the HSN cell bodies might contribute to the observed guidance defects, we scored HSN pathfinding in animals with wild-type and misplaced HSN neurons separately (Fig. 3I, Table 1). We found that crossover defects occurred in both cases, but were indeed more frequent in animals with mispositioned HSN cell bodies.

### Commissures of ventral nerve cord motoneurons

Midline decisions are also made by different types of motoneurons in the VNC. In the case of D-type motoneurons (DD and VD subtypes), axons extend first in the right VNC and then circumferentially grow out on the right side of the animal (with the exception of the two anteriormost DD and VD neurons, which grow out on the left) to form the commissures that connect to the dorsal nerve cord (DNC; Fig. 4A). The axons of the six DD neurons grow out during embryonic development, whereas those of the 13 VD neurons grow out postembryonically. We analyzed *sdn-1(zh20)* and *sdn-1(ok449)* mutants for two major guidance defects: first, the circumferential guidance to the DNC; and, second, the left/right decision during the exit from the VNC (Fig. 4E). In wild-type worms, the commissural axons always reach the DNC where they bifurcate and connect to neighboring branches of the D-type motoneurons to form a continuous DNC fascicle (Fig. 4C,E). In both *sdn-1* mutants, the circumferential outgrowth of commissures was impaired,

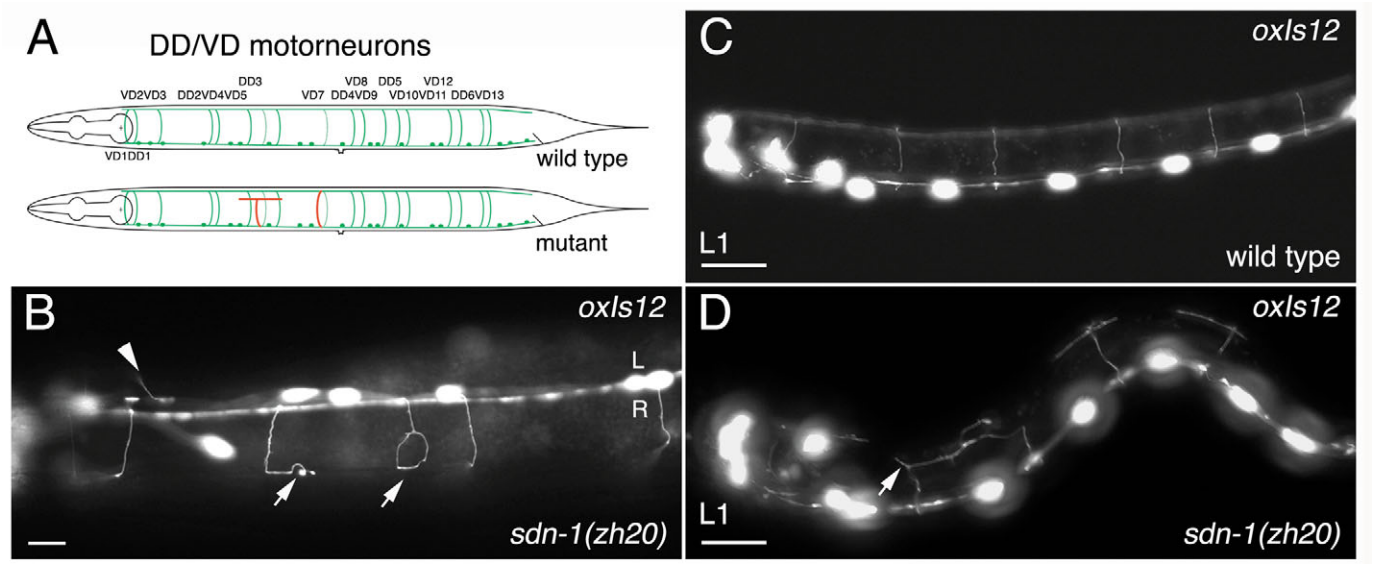


E

% commissural reach (circumf. elong) 1.

| | left | N | right | N |
|---|---|---|---|---|
| wild type | 100 | 23 | 100 | 460 |
| *sdn-1(zh20)* | 75 | 110 | 92 | 674 |
| *sdn-1(ok449)* | 84 | 110 | 97 | 698 |
| *hst-6(ok273)* | 91 | 32 | 99 | 278 |
| *sdn-1(zh20) hst-6(ok273)* | 40 | 161 | 75 | 633 |
| *hse-5(tm472)* | 30 | 223 | 78 | 507 |
| *hse-5(tm472); sdn-1(zh20)* | 14 | 217 | 20 | 417 |

% animals with n inappropriate commissures on the left L/R 2.

| 0 | 1 | 2 | 3 | 4 | 5 | 6 | 7 | 8 | N |
|---|---|---|---|---|---|---|---|---|---|
| 76 | 20 | 3 | 1 | 0 | 0 | 0 | 0 | 0 | 93 |
| 11 | 21 | 29 | 20 | 9 | 8 | 2 | 0 | 0 | 135 |
| 12 | 24 | 26 | 16 | 18 | 2 | 2 | 0 | 0 | 50 |
| 22 | 39 | 20 | 12 | 7 | 0 | 0 | 0 | 0 | 50 |
| 2 | 10 | 16 | 23 | 23 | 10 | 10 | 5 | 1 | 135 |
| 0 | 1 | 7 | 15 | 19 | 28 | 17 | 11 | 2 | 87 |
| 0 | 2 | 22 | 18 | 10 | 20 | 14 | 8 | 6 | 50 |

**Fig. 4.** Loss of SDN-1 affects the guidance and left/right choices of commissural motoneurons. (A) Schematic of DD and VD motoneurons. (B,E) DD/VD commissures in young adults and (C,D) embryonic DD commissures in the L1 larva. (B) Ventral nerve cord (VNC) view of an *sdn-1(zh20)* animal. D-type motoneurons inappropriately grow out on the left side of the animal (arrowhead) or stop prematurely before reaching the dorsal nerve cord (DNC) (arrows). L, left side; R, right side. (C) Six DD commissures form a continuous dorsal nerve cord in the wild-type L1 larva. (D) In *sdn-1* null mutants, DD commissures branch prematurely and fail to reach the DNC (arrow). (E) D-type motoneuron development analyzed for: (1) circumferential outgrowth of DD/VD commissures to the DNC; (2) left/right choice to exit the VNC. (1) N represents the total number of commissures scored. Right and left denote the percentage of commissures that reach the DNC when growing out on the correct (right side) and incorrect side (left side), respectively. Note that guidance is considerably more affected if axons grow out on the wrong side of the animal. (2) N represents the number of animals analyzed. Each column gives the percentage of animals that show the indicated amount (1-8) of commissures inappropriately exiting the VNC on the left side. Scale bars: 10 μm.

especially on the left side of the worm (Fig. 4B,D,E). Furthermore, *sdn-1* mutants showed partial VNC defasciculation and an increased number of commissures inappropriately leaving the VNC on the left side (Fig. 4E, Table 1). The outgrowth of other types of neurons, such as the sensory neurons in the head or the pioneering axons in the VNC, were not affected in *sdn-1(zh20)* null mutants (Table 1).

Taken together, our findings indicate that syndecan SDN-1 is required for several distinct axon guidance and cellular migration events. Interestingly, the *sdn-1(zh20)* axon guidance defects that we describe here are similar to those previously reported in mutants for the HS-modifying enzymes (Bülow and Hobert, 2004), suggesting that SDN-1 might be a major target of these enzymes in the developing nervous system. Moreover, animals expressing the truncated form of syndecan lacking the major HS attachment sites showed qualitatively and quantitatively similar defects to those observed in syndecan null mutants, pointing to a major role of the HS moiety of SDN-1 in regulating cell migration and axonal pathfinding.

## SDN-1 is highly expressed in the nervous system

In order to examine the expression pattern of SDN-1, we generated transgenic animals expressing a full-length C-terminally tagged SDN-1::GFP fusion protein. In embryos and L1 larvae, SDN-1::GFP was expressed in many tissues, including neurons, pharynx and hypodermis (Fig. 5A′). In later larval stages and in adult worms, SDN-1::GFP was predominantly expressed in the nervous system, with strong expression in the nerve ring and the VNC motoneurons (Fig. 5B,C,E,F). Apart from the neuronal expression, SDN-1::GFP was also found at a lower level in the hypodermis (Fig. 5D) and the vulval cells (data not shown). Because antibodies directed against the conserved intracellular domain of mammalian syndecan 4 have been reported to specifically detect *C. elegans* SDN-1 in the nerve ring and the vulva (Minniti et al., 2004), the SDN-1::GFP reporter likely reflects the endogenous SDN-1 expression pattern.

## SDN-1 functions in neurons to control cell migration and axon guidance

Based on the SDN-1::GFP expression pattern, it is conceivable that SDN-1 could affect neuronal differentiation in a cell non-autonomous manner. In particular, SDN-1 expressed in the hypodermis might regulate the diffusion and thus spatial distribution of secreted guidance cues. Alternatively, SDN-1 might function cell autonomously in the migrating neurons and navigating growth cones to modulate – possibly through its HS chains – the interaction of specific ligand/receptor pairs.

To distinguish between these two possibilities, we expressed a full-length *sdn-1* cDNA under the control of either the hypodermal *dpy-7* promoter ($P_{dpy\text{-}7}$*::sdn-1*) (Gilleard et al., 1997) or the pan-neuronal *unc-119* promoter (Maduro et al., 2000), and tested the rescuing activity of the different transgenes. Interestingly, neuron-specific expression of SDN-1, as well as expression of SDN-1 driven by the endogenous *sdn-1* promoter ($P_{sdn\text{-}1}$*::sdn-1*) rescued the HSN and ALM migration defects of *sdn-1* null mutants (Table 2). By contrast, hypodermal expression of SDN-1 under control of the *dpy-7* promoter had no significant effect on ALM migration, although it did weakly reduce the HSN migration defects (Table 2).

To determine whether cell type-specific expression of SDN-1 was sufficient to rescue the axon guidance defects of the corresponding neurons, we expressed SDN-1 under the PVQ-specific *sra-6* promoter ($P_{sra\text{-}6}$*::sdn-1*). PVQ-specific expression of SDN-1 significantly reduced the crossover defects of PVQ interneurons, with a similar efficiency as expression of SDN-1 under its endogenous promoter (Table 3). By contrast, expression of SDN-1 in hypodermal tissue ($P_{dpy\text{-}7}$*::sdn-1*) showed no rescuing activity. In summary, our data indicate that SDN-1 is likely to act cell autonomously in neurons to promote cell migration and axonal pathfinding.

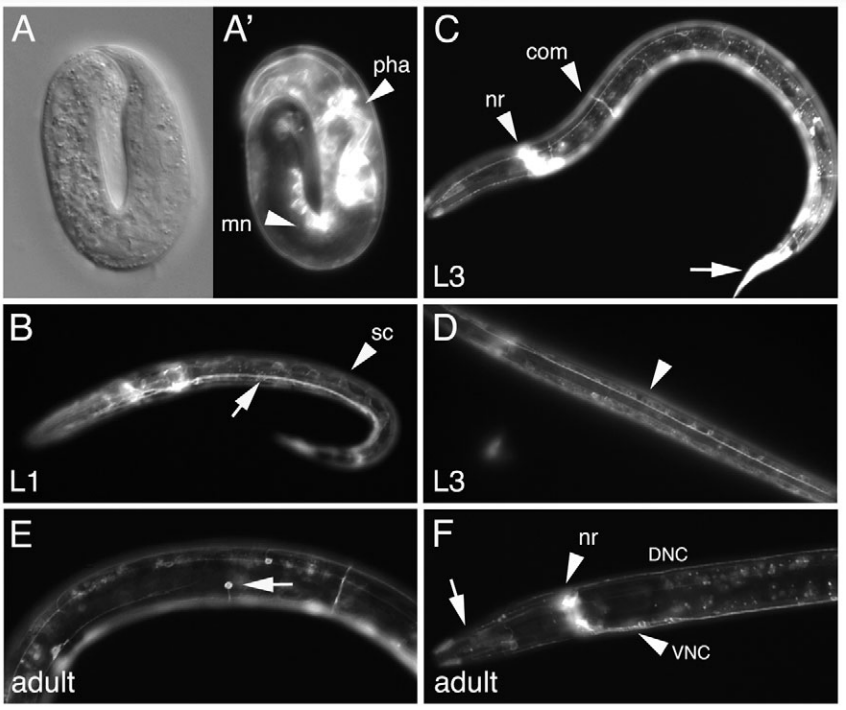


**Fig. 5.** SDN-1 expression in neural and hypodermal tissue. (A-F) Expression pattern of the translational $P_{sdn\text{-}1}$*::sdn-1::gfp* reporter. (A′) SDN-1::GFP is broadly expressed in the three-fold embryo, and is particularly strong in the pharynx (pha) and the motoneurons (mn) of the VNC. (B) In L1 larvae, expression is seen in the VNC (arrow) and around the seam cells (arrowhead). SDN-1::GFP expression is also visible in embryonic DD commissures (out of focal plane in B). (C) During later larval stages, SDN-1::GFP is predominantly found in the nervous system. The nerve ring (nr), and the VNC motoneurons and commissures (com) show the highest expression levels (arrowheads; B,F), but the reporter is also present in touch neurons (arrow; E) and other sensory neurons in the head (arrow; F). SDN-1::GFP can also be detected at a lower level in the body wall hypodermis (arrowhead; D); expression is stronger in hypodermal tissue in the tail (arrow; C).

**Table 2. Rescue of cell migration defects**

| Genotype | Transgene expression | % Defective HSN | *n* |
|---|---|---|---|
| **A. HSN migration** | | | |
| Wild type | N/A | 0 | 50 |
| *sdn-1(zh20)* | N/A | 55±3 | 52 |
| *sdn-1(zh20); opEx1216* [$P_{sdn\text{-}1}$*::sdn-1*] | Hypodermis, neurons | 13±2 | 62 |
| *sdn-1(zh20); opEx1217* [$P_{sdn\text{-}1}$*::sdn-1*] | Hypodermis, neurons | 13±3 | 46 |
| *sdn-1(zh20); opEx1218* [$P_{sdn\text{-}1}$*::sdn-1*] | Hypodermis, neurons | 14±2 | 77 |
| *sdn-1(zh20); opEx1221* [$P_{unc\text{-}119}$*::sdn-1*] | Pan-neuronal | 4±1 | 75 |
| *sdn-1(zh20); opEx1222* [$P_{unc\text{-}119}$*::sdn-1*] | Pan-neuronal | 3±1 | 68 |
| *sdn-1(zh20); opEx1224* [$P_{unc\text{-}119}$*::sdn-1*] | Pan-neuronal | 7±2 | 82 |
| *sdn-1(zh20); opEx1226* [$P_{dpy\text{-}7}$*::sdn-1*] | Hypodermis | 40±3 | 78 |
| *sdn-1(zh20); opEx1227* [$P_{dpy\text{-}7}$*::sdn-1*] | Hypodermis | 35±2 | 130 |
| *sdn-1(zh20); opEx1230* [$P_{dpy\text{-}7}$*::sdn-1*] | Hypodermis | 31±3 | 64 |

| Genotype | Transgene expression | % Defective ALM | *n* |
|---|---|---|---|
| **B. ALM migration** | | | |
| Wild type | N/A | 0±1 | 100 |
| *sdn-1(zh20)* | N/A | 42±3 | 96 |
| *sdn-1(zh20); opEx1196* [$P_{sdn\text{-}1}$*::sdn-1*] | Hypodermis, neurons | 19±2 | 68 |
| *sdn-1(zh20); opEx1198* [$P_{sdn\text{-}1}$*::sdn-1*] | Hypodermis, neurons | 10±2 | 69 |
| *sdn-1(zh20); opEx1199* [$P_{sdn\text{-}1}$*::sdn-1*] | Hypodermis, neurons | 13±2 | 85 |
| *sdn-1(zh20); opEx1206* [$P_{unc\text{-}119}$*::sdn-1*] | Pan-neuronal | 5±1 | 82 |
| *sdn-1(zh20); opEx1207* [$P_{unc\text{-}119}$*::sdn-1*] | Pan-neuronal | 9±2 | 80 |
| *sdn-1(zh20); opEx1208* [$P_{unc\text{-}119}$*::sdn-1*] | Pan-neuronal | 6±1 | 82 |
| *sdn-1(zh20); opEx1202* [$P_{dpy\text{-}7}$*::sdn-1*] | Hypodermis | 51±4 | 43 |
| *sdn-1(zh20); opEx1204* [$P_{dpy\text{-}7}$*::sdn-1*] | Hypodermis | 51±3 | 63 |
| *sdn-1(zh20); opEx1205* [$P_{dpy\text{-}7}$*::sdn-1*] | Hypodermis | 32±3 | 50 |

### *sdn-1* interacts genetically with genes encoding HS-modifying enzymes in a context-dependent manner

We next investigated whether we could identify specific modification patterns of HS chains carried by SDN-1 that could confer to the axons the ability to selectively respond to midline guidance cues. To address this issue, we examined double-null mutants between *sdn-1(zh20)* and mutants in the HS-modifying enzymes. As the C5-epimerase HSE-5 and the 2*O*-sulfotransferase HST-2 have previously been shown to act in the same pathway for midline guidance, we concentrated our analysis on HSE-5 and the 6*O*-sulfotransferase HST-6 (Bülow and Hobert, 2004).

For D-type motoneurons, we found that in animals lacking both HSE-5 and SDN-1 the outgrowth of commissures to the DNC was drastically reduced compared with that of either single mutant (Fig. 6A-D′). Moreover, *hse-5; sdn-1* double null mutant L1 larvae showed a highly defasciculated VNC (Fig. 6C′) and most of the embryonic DD commissures failed to reach the DNC (Fig. 6A,B′). We observed a similar range of defects in L4 larvae and adult animals, where most of the DD and VD commissures were misguided and did not connect to the DNC (Fig. 6D′).

Similarly, *sdn-1 hst-6* double-null mutants (L1 larvae and adults) showed more severe phenotypes in D-type motoneurons than did either single mutant alone, but the increase of defects was less pronounced than in *hse-5; sdn-1* double-null worms (Fig. 6A, Fig. 4E). The strong enhancement of the guidance defects observed in *hse-5; sdn-1* double mutants suggests that HSE-5 acts in parallel with SDN-1, i.e. that HSE-5 must modify at least one additional HSPG regulating a parallel signaling pathway. Because *sdn-1 hst-6* double mutants show a detectable enhancement of guidance defects in D-type motoneurons when compared with either single mutant, SDN-1 may not be the only substrate of HST-6 in D-type motoneurons.

To expand these observations in a different cellular context, we also examined the pathfinding of PVQ interneurons. Again, *hse-5; sdn-1* double-null animals showed significantly more

**Table 3. Rescue of PVQ guidance defects**

| Genotype | Transgene expression | % Defective PVQ | *n* |
|---|---|---|---|
| Wild type | N/A | 9±2 | 142 |
| *sdn-1(zh20)* | N/A | 49±4 | 140 |
| *sdn-1(zh20); opEx1159* [$P_{dpy7}$*::sdn-1*] | Hypodermis | 58±4 | 128 |
| *sdn-1(zh20); opEx1160* [$P_{dpy7}$*::sdn-1*] | Hypodermis | 58±5 | 112 |
| *sdn-1(zh20); opEx1161* [$P_{dpy7}$*::sdn-1*] | Hypodermis | 50±5 | 122 |
| *sdn-1(zh20); opEx1162* [$P_{sra\text{-}6}$*::sdn-1*] | PVQ interneurons | 22±4 | 111 |
| *sdn-1(zh20); opEx1163* [$P_{sra\text{-}6}$*::sdn-1*] | PVQ interneurons | 25±4 | 111 |
| *sdn-1(zh20); opEx1164* [$P_{sra\text{-}6}$*::sdn-1*] | PVQ interneurons | 30±4 | 109 |
| *sdn-1(zh20); opEx1165* [$P_{sdn\text{-}1}$*::sdn-1*] | Hypodermis, neurons | 37±5 | 111 |
| *sdn-1(zh20); opEx1166* [$P_{sdn\text{-}1}$*::sdn-1*] | Hypodermis, neurons | 18±4 | 109 |
| *sdn-1(zh20); opEx1167* [$P_{sdn\text{-}1}$*::sdn-1*] | Hypodermis, neurons | 23±4 | 109 |

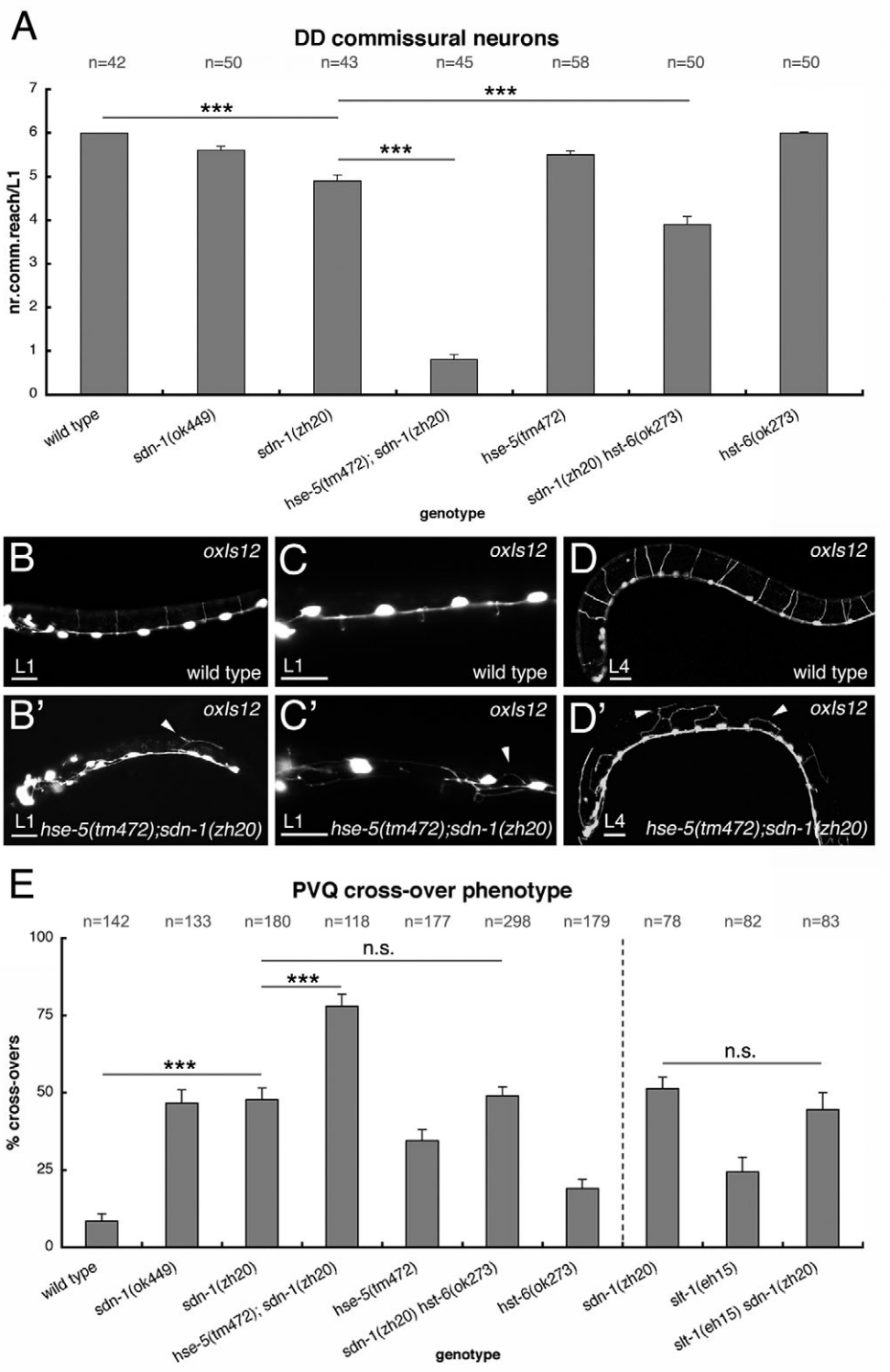


**Fig. 6.** Double mutant analysis of SDN-1 and HS-modifying enzymes. (A) Circumferential guidance of DD commissures (L1 larvae), as shown by the genetic interaction of *sdn-1* nulls with HS-modifying enzyme mutants. Data represent the number of commissures that reach the level of the DNC per L1 larva. Error bars indicate s.e.m. (B,B′) Analysis of DD commissures in L1 larvae. (B′) In *hse-5; sdn-1* double-null mutants, most DD commissures either fail to grow out dorsally or branch prematurely (arrowhead). (C,C′) VNC view of L1 larvae. (C′) The VNC of *hse-5; sdn-1* double-null mutants is highly defasciculated (arrowhead). (D,D′) DD/VD commissures of L4 larvae. (D′) Circumferential guidance of DD/VD motoneurons is disrupted in *hse-5*; *sdn-1* double mutants (arrowheads). D and D′ show confocal *z*-stack images to visualize all misguided commissures in different focal planes. (E) The PVQ crossover phenotype demonstrated by the genetic interactions of *sdn-1* null worms with HS-modifying enzyme mutants and *slt-1(eh15)*. Error bars indicate the standard error of proportion. Asterisks denote statistical significance as follows: ***$P$<0.0001; n.s., not significant; *n*, number of animals scored. Scale bars: 10 μm in B-C′; 25 μm in D,D′.

PVQ crossover defects than did either single mutant (Fig. 6E). In most *hse-5; sdn-1* worms, midline crossing had already occurred in the posterior region, leading to completely collapsed PVQ tracts (>50% of crossover defects). In contrast to D-type motoneurons, loss of HST-6 function did not result in a statistically significant enhancement of the *sdn-1* null phenotype. Interestingly, HST-6 is predominantly expressed in neurons, in contrast to HSE-5, which is mainly expressed in the hypodermis (Bülow and Hobert, 2004). This finding, together with our observation that loss of HST-6 function does not lead to more severe PVQ crossover defects in an *sdn-1* null background, suggests that 6*O*-sulfated HS, generated by HST-6, is important for SDN-1 function in PVQ midline crossing. By contrast, in D-type motoneurons, both *hse-5*; *sdn-1* and *sdn-1 hst-6* double-null mutants exhibited additive effects. Thus, signaling in different cellular contexts (D-type motoneurons

versus PVQ) might depend on a different combination of HS modifications.

In summary, the epistasis analysis with HS-modifying enzyme mutants points to the existence of a parallel, SDN-1-independent midline guidance pathway modulated by a distinct HSPG core protein that is a major target of the sugar epimerase HSE-5. Although our results do not exclude the possibility that HSE-5 also modifies SDN-1, the fact that *sdn-1(zh20)* enhances the *hse-5* loss-of-function phenotype indicates that, even in the absence of C5-epimerization, SDN-1 still regulates axon guidance.

### SDN-1 acts in the Slit/Robo pathway

As the above experiment showed that syndecan SDN-1 is required for midline guidance, we speculated that SDN-1 might act as a co-receptor in one of the known axon guidance pathways, such as UNC-6/Netrin or Slit/Robo (Hao et al., 2001; Ishii et al., 1992; Zallen et al., 1998). The *C. elegans* genome encodes one Robo receptor (SAX-3) and one Slit homolog (SLT-1), which are both required for ventral axon guidance (Hao et al., 2001). Furthermore, interneurons that are usually separated in the left and right VNC inappropriately cross the midline in *sax-3* and *slt-1* mutants (Hao et al., 2001), a defect similar to the phenotype that we observed in *sdn-1* mutants.

In order to test whether SDN-1 acts in the SLT-1-dependent signaling pathway, we used the presumptive null allele *slt-1(eh15)* (Hao et al., 2001) and compared the phenotype of *slt-1 sdn-1* double-null mutants with that of either single mutant (Fig. 6E). The midline crossing defects in *slt-1 sdn-1* double mutants were no more severe than those of either single mutant, suggesting that SDN-1 acts in the same genetic pathway as SLT-1. Likewise, *slt-1 sdn-1* double mutants did not show enhanced defects of L/R choices of D-type motoneurons (data not shown).

## Discussion

The differential modification of HS sugar chains was recently found to be required for various aspects of axon guidance. This observation led to the development of the 'sugar-code hypothesis' (Bülow and Hobert, 2004), which states that tissue-specific sugar side-chain modifications, like tissue-specific alternative splicing or tissue-specific heterodimerization, can modulate and fine-tune the activity of a core protein (in this case the HSPGs). In this study, we show that the HSPG core protein SDN-1 acts autonomously in neurons to direct cell migration and specify axon guidance decisions at the midline. We provide evidence that distinct modification patterns on SDN-1 and at least one additional HSPG core protein allow these proteins to differentially modulate two partially redundant axon guidance signaling pathways.

### Syndecan in cell migration

Loss of SDN-1 function interferes with the migration of the HSN, CAN and ALM neurons, which, together with Q neuroblasts, are the only groups of neurons that migrate long distances in *C. elegans*. Because similar ALM migration defects have been reported for mutations in *sax-3*/Robo (Zallen et al., 1999), SDN-1 might also modulate Slit/Robo signaling in cell migration, in addition to its role in the regulation of Slit signaling in midline guidance indicated by our data. However, lack of SDN-1 does not perturb cell migration in general; for example, sex myoblast migration is normal in *sdn-1(zh20)* animals (data not shown). Furthermore, *sdn-1* null mutants exhibit no circumferential distal tip cell (DTC) migration defects. Mutations in the gene encoding perlecan/UNC-52, a basement membrane HSPG, enhance the DTC migration defects of UNC-6/netrin signaling mutants – an effect that can be partially suppressed by mutations disrupting growth factor-like signaling (Merz et al., 2003). Whether SDN-1 also contributes to signaling by EGL-20/WNT, UNC-129/TGF-β or EGL-17/FGF still needs to be determined.

Another candidate pathway that could be regulated by SDN-1 is signaling by integrins. *C. elegans ina-1* α integrin was shown to be required in neurons for the migration of HSN, ALM and CAN neurons (Baum and Garriga, 1997). Intriguingly, *ina-1* mutants also show defects in coelomocyte migration, whereas sexmyoblast migration is normal, similar to the situation we found in *sdn-1(zh20)* null mutants. In addition, cell culture studies have demonstrated a crucial role of the syndecan extracellular domain in regulating the adhesion and invasion of tumor cells, possibly by interacting with integrins (Beauvais et al., 2004; Burbach et al., 2004). Understanding the role of syndecan in cell migration is particularly relevant in light of the role mammalian syndecans play during carcinogenesis. Upregulation of human syndecan 1 in breast and pancreatic cancer, for example, usually correlates with more invasive tumors, although, in other types of cancer, downregulation of syndecan seems to have equally adverse effects (Beauvais and Rapraeger, 2004; Leivonen et al., 2004). In *C. elegans*, SDN-1 could promote cell migration either by modulating the activity of guidance cues or, directly, by regulating cell adhesion.

### Syndecan in axon guidance

How might SDN-1 function in axon guidance? A recent study in *Drosophila* has shown that loss of syndecan function affects the extracellular distribution of the ligand Slit, which is secreted by midline cells and might therefore interfere with signal transduction by Robo receptors (Johnson et al., 2004). Neural expression of *Drosophila* syndecan rescued the guidance defects of syndecan mutant flies, whereas the expression of syndecan in midline cells did not (Johnson et al., 2004).

Similarly, our data suggest that *C. elegans* SDN-1 functions in neurons to ensure the correct midline guidance of axons. Cell type-specific expression of SDN-1 in PVQ interneurons partially rescued the midline pathfinding errors of these cells, whereas expression of SDN-1 in the surrounding epidermis failed to rescue. Incomplete rescue of PVQ crossovers, also seen for SDN-1 driven by its endogenous promoter, could be explained by insufficient expression of the rescuing arrays in PVQ neurons due to the lack of an enhancer sequence in the promoters that we used.

Neuronal SDN-1 could act as a co-receptor of specific axon guidance receptors and might thereby enhance the efficacy of the signaling event (quantitative modulation), alter the specificity of the ligand/receptor interaction (qualitative modulation), or both. One good candidate for a receptor that may require SDN-1 for ligand binding is the Slit/SLT-1 receptor SAX-3. *sdn-1* mutants show similar pathfinding errors

as *slt-1* or *sax-3* mutants, and genetic epistasis analysis placed *sdn-1* in the same genetic pathway as *slt-1* in certain cellular contexts (PVQ and D-type motoneuron development).

Alternatively, SDN-1, being a transmembrane protein, could also act directly as a receptor and generate an intracellular signal on its own. For example, *Xenopus* syndecan 2 participates in inside-out signaling that specifies the left-right looping of the heart and gut, which is mediated by PKCγ phosphorylation of the syndecan cytoplasmic domain (Kramer et al., 2002). Beyond their function as (co-)receptors, syndecans may also be involved in the targeting of guidance receptors to specific membrane compartments, such as lipid rafts (Couchman, 2003).

The C terminus of mammalian syndecans has been shown to interact with the PDZ domain of the membrane-associated guanylate kinase CASK (Cohen et al., 1998; Hsueh et al., 1998). The *C. elegans* CASK homolog LIN-2 is required together with LIN-7 and LIN-10 for the basolateral localization of the EGF receptor on vulval precursor cells (Kaech et al., 1998). SDN-1 might therefore be required to anchor the LIN-2/LIN-7/LIN-10 complex to the basolateral plasma membrane and thereby localize the EGF/LET-23 receptor. Although SDN-1::GFP is present on the basolateral side of the primary vulval cells (data not shown), loss of SDN-1 had no effect on EGF receptor localization. However, these observations do not exclude a possible role for SDN-1 in the targeting of axon guidance receptors.

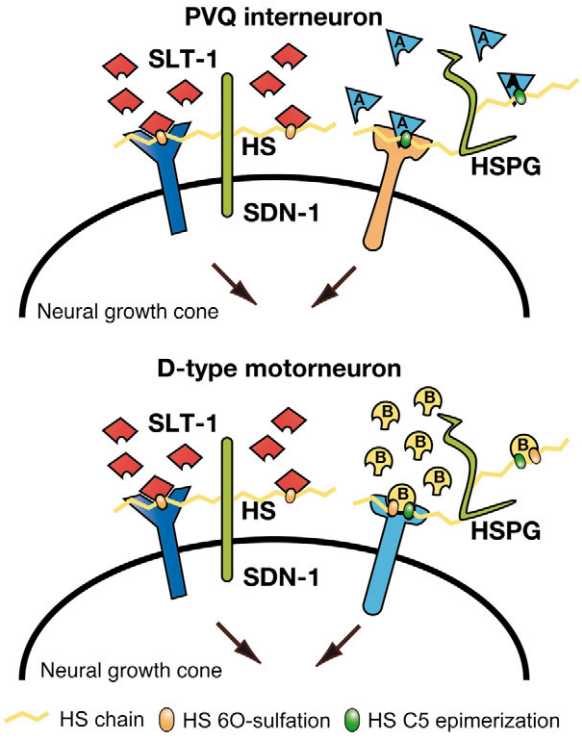


**Fig. 7.** Model for syndecan function in axon guidance signaling. Syndecan (SDN-1) on the neural growth cone exposes HS chains with 'neuron-specific' sugar modifications, here simplified by 6*O*-sulfations. The HS side chains of syndecan bind specific guidance cues (e.g. SLT-1) and modulate signaling by cognate high-affinity receptors, such as the SAX-3/Robo receptor (co-receptor function). Genetic analysis suggests that parallel signaling to syndecan relies on distinct sugar motifs on additional HSPGs in a context-dependent manner. In PVQ interneurons, this parallel pathway involves HS with epimerization (green), whereas in motoneuron development it involves both epimerization and 6*O*-sulfation. The HS modification patterns may thus define the specificity of different ligand/receptor interactions; A and B represent different ligands.

## Syndecan and specific HS modifications

Interestingly, *sdn-1(zh20)* null animals showed comparable phenotypes for PVQ guidance and HSN migration to *sdn-1(ok449)* mutants, which express a mutant SDN-1 lacking the major HS side chains. This observation underlines the importance of the HS side chains and the information encoded in their sugar modifications for correct axon guidance, although it is possible that conformational changes due to the deleted region in the ectodomain or an altered distribution of the truncated SDN-1 form account for the defects observed in *sdn-1(ok449)* mutants. Importantly, we have found that SDN-1 is not the only HSPG controlling the axon guidance of PVQ interneurons and VNC motoneurons. Based on our epistasis analysis, we predict the existence of an additional axon guidance pathway, which relies on HS modifications by the C5-epimerase HSE-5, or on both HSE-5 and the 6*O*-sulfotransferase HST-6 – depending on the cellular context (Fig. 7). As it was shown that HSE-5 acts in the epidermis (Bülow and Hobert, 2004), this parallel pathway may depend on C5-epimerized HS sugars on a, as yet to be identified, HSPG expressed by the surrounding epidermal cells.

*C. elegans* mutant for glypican GPN-1, the second major cell surface HSPG, do not seem to display axon guidance or cell migration defects (Hannes Bülow and Oliver Hobert, personal communication). In all events that we analyzed (PVQ and DD/VD guidance, HSN migration), *gpn-1(ok377)* failed to enhance the defects of *sdn-1(zh20)* null animals (data not shown), indicating that HSE-5 might modify an extracellular or as yet unknown cell surface HSPG. The UNC-6/Netrin and VAB-1/Ephrin guidance systems act in parallel with SLT-1/Slit signaling to define midline guidance (Zallen et al., 1999), and are thus candidate pathways to be regulated by such proposed epimerized sugar motifs on a HSPG core protein distinct from SDN-1.

In PVQ interneurons, lack of the 6*O*-sulfotransferase HST-6 in worms devoid of SDN-1 did not cause a significant enhancement of crossover defects when compared with *sdn-1* single mutants. Thus, the HS side chains on SDN-1 are likely to be important substrates of HST-6 in PVQ (Fig. 7). HST-6 is, however, also involved in SDN-1-independent signaling, in the context of D-type motoneuron guidance.

## Regulation by specific sugar modifications

Our results provide further evidence for the existence of a 'sugar code' on cell-surface and extracellular HSPGs that regulates the differential responses of axons towards the various extracellular guidance cues that they normally encounter. For example, 6*O*-sulfated HS side chains may act as 'molecular antennae' on SDN-1 to enhance the perception of Slit signals, as well as a modulator for the ligand/receptor interaction, while the input from parallel guidance systems could be regulated by extracellular HSPGs carrying C5-epimerized HS chains, with or without 6*O*-sulfation (Fig. 7). In this way, the sensitivity of axons towards Slit signals could be dynamically regulated

through the combinatorial control of HS-modifying enzyme expression and cell surface exposure of SDN-1. Indeed, during an early phase of mouse brain development, the different syndecan family members, as well as the HS-modifying enzymes, show tightly regulated spatiotemporal expression patterns (Ford-Perriss, 2003; Sedita et al., 2004).

The fact that HSPGs are highly conserved from nematodes to humans supports the idea that tissue-specific HS sugar modifications of HSPGs are a key factor that determines the cellular specificity of the different axon guidance systems (Hutter et al., 2000). Rules learned in *C. elegans* are thus likely to also apply in mammals, and promise to lead to a better understanding of the mechanisms that regulate nervous system development.

We thank Hannes Bülow and Oliver Hobert for stimulating discussions and sharing results prior to publication. We thank the CGC and various *C. elegans* researchers for providing strains and markers, the *C. elegans* Knockout Consortium in Oklahoma for providing deletion mutants, Eduardo Moreno and members of the Hengartner and Hajnal laboratories for comments on the manuscript, and Amit Dutt and Doris Klingele for technical support. This work was funded by the Swiss National Science Foundation (M.O.H. and A.H.), the Forschungskredit of the University of Zurich (C.R.) and the Ernst Hadorn Foundation (M.O.H.).

## References

**Ackley, B. D., Crew, J. R., Elamaa, H., Pihlajaniemi, T., Kuo, C. J. and Kramer, J. M.** (2001). The NC1/endostatin domain of *Caenorhabditis elegans* type XVIII collagen affects cell migration and axon guidance. *J. Cell Biol.* **152**, 1219-1232.

**Baum, P. D. and Garriga, G.** (1997). Neuronal migrations and axon fasciculation are disrupted in *ina-1* integrin mutants. *Neuron* **19**, 51-62.

**Beauvais, D. M. and Rapraeger, A. C.** (2004). Syndecans in tumor cell adhesion and signaling. *Reprod. Biol. Endocrinol.* **2**, 1-12.

**Beauvais, D. M., Burbach, B. J. and Rapraeger, A. C.** (2004). The syndecan-1 ectodomain regulates alphavbeta3 integrin activity in human mammary carcinoma cells. *J. Cell Biol.* **167**, 171-181.

**Bernfield, M., Gotte, M., Park, P. W., Reizes, O., Fitzgerald, M. L., Lincecum, J. and Zako, M.** (1999). Functions of cell surface heparan sulfate proteoglycans. *Annu. Rev. Biochem.* **68**, 729-777.

**Berset, T., Hoier, E. F., Battu, G., Canevascini, S. and Hajnal, A.** (2001). Notch inhibition of RAS signaling through MAP kinase phosphatase LIP-1 during *C. elegans* vulval development. *Science* **291**, 1055-1058.

**Bornemann, D. J., Duncan, J. E., Staatz, W., Selleck, S. and Warrior, R.** (2004). Abrogation of heparan sulfate synthesis in *Drosophila* disrupts the Wingless, Hedgehog and Decapentaplegic signaling pathways. *Development* **131**, 1927-1938.

**Brenner, S.** (1974). The genetics of *Caenorhabditis elegans*. *Genetics* **77**, 71-94.

**Bülow, H. E. and Hobert, O.** (2004). Differential sulfations and epimerization define heparan sulfate specificity in nervous system development. *Neuron* **41**, 723-736.

**Bülow, H. E., Berry, K. L., Topper, L. H., Peles, E. and Hobert, O.** (2002). Heparan sulfate proteoglycan-dependent induction of axon branching and axon misrouting by the Kallmann syndrome gene kal-1. *Proc. Natl. Acad. Sci. USA* **99**, 6346-6351.

**Burbach, B. J., Ji, Y. and Rapraeger, A. C.** (2004). Syndecan-1 ectodomain regulates matrix-dependent signaling in human breast carcinoma cells. *Exp. Cell Res.* **300**, 234-247.

**Chan, S. S., Zheng, H., Su, M. W., Wilk, R., Killeen, M. T., Hedgecock, E. M. and Culotti, J. G.** (1996). UNC-40, a *C. elegans* homolog of DCC (Deleted in Colorectal Cancer), is required in motile cells responding to UNC-6 netrin cues. *Cell* **87**, 187-195.

**Cohen, A. R., Woods, D. F., Marfatia, S. M., Walther, Z., Chishti, A. H. and Anderson, J.** (1998). Human CASK/LIN-2 binds syndecan-2 and protein 4.1 and localizes to the basolateral membrane of epithelial cells. *J. Cell Biol.* **142**, 129-138.

**Couchman, J. R.** (2003). Syndecans: proteoglycan regulators of cell-surface microdomains? *Nat. Rev. Mol. Cell. Biol.* **4**, 926-937.

**Esko, J. D. and Selleck, S. B.** (2002). Order out of chaos: assembly of ligand binding sites in heparan sulfate. *Annu. Rev. Biochem.* **71**, 435-471.

**Ford-Perriss, M., Turner, K., Guimond, S., Apedaile, A., Haubeck, H. D., Turnbull, J. and Murphy, M.** (2003). Localisation of specific heparan sulfate proteoglycans during the proliferative phase of brain development. *Dev. Dyn.* **227**, 170-184.

**Gilleard, J. S., Barry, J. D. and Johnstone, I. L.** (1997). cis regulatory requirements for hypodermal cell-specific expression of the *Caenorhabditis elegans* cuticle collagen gene *dpy-7*. *Mol. Cell. Biol.* **17**, 2301-2311.

**Halfter, W., Dong, S., Schurer, B. and Cole, G. J.** (1998). Collagen XVIII is a basement membrane heparan sulfate proteoglycan. *J. Biol. Chem.* **273**, 25404-25412.

**Hao, J. C., Yu, T. W., Fujisawa, K., Culotti, J. G., Gengyo-Ando, K., Mitani, S., Moulder, G., Barstead, R., Tessier-Lavigne, M. and Bargmann, C. I.** (2001). *C. elegans* slit acts in midline, dorsal-ventral, and anterior-posterior guidance via the SAX-3/Robo receptor. *Neuron* **32**, 25-38.

**Hartmann, U. and Maurer, P.** (2001). Proteoglycans in the nervous system – the quest for functional roles in vivo. *Matrix Biol.* **20**, 23-35.

**Hedgecock, E. M., Culotti, J. G., Hall, D. H. and Stern, B. D.** (1987). Genetics of cell and axon migrations in *Caenorhabditis elegans*. *Development* **100**, 365-382.

**Herman, T., Hartwieg, E. and Horvitz, H. R.** (1999). sqv mutants of *Caenorhabditis elegans* are defective in vulval epithelial invagination. *Proc. Natl. Acad. Sci. USA* **96**, 968-973.

**Hobert, O.** (2002). PCR fusion-based approach to create reporter gene constructs for expression analysis in transgenic *C. elegans*. *Biotechniques* **32**, 728-730.

**Hsueh, Y. P., Yang, F. C., Kharazia,V., Naisbitt, S., Cohen, A. R., Weinberg, R. J. and Sheng, M.** (1998). Direct interaction of CASK/LIN-2 and syndecan heparan sulfate proteoglycan and their overlapping distribution in neuronal synapses. *J. Cell Biol.* **142**, 139-151.

**Hutter, H., Vogel, B. E., Plenefisch, J. D., Norris, C. R., Proenca, R. B., Spieth, J., Guo, C., Mastwal, S., Zhu, X., Scheel, J. et al.** (2000). Conservation and novelty in the evolution of cell adhesion and extracellular matrix genes. *Science* **287**, 989-994.

**Inatani, M., Irie, F., Plump, A. S., Tessier-Lavigne, M. and Yamaguchi, Y.** (2003). Mammalian brain morphogenesis and midline axon guidance require heparan sulfate. *Science* **302**, 1044-1046.

**Ishii, N., Wadsworth, W. G., Stern, B. D., Culotti, J. G. and Hedgecock, E. M.** (1992). UNC-6, a laminin-related protein, guides cell and pioneer axon migrations in *C. elegans*. *Neuron* **9**, 873-881.

**Jansen, G., Hazendonk, E., Thijssen, K. L. and Plasterk, R. H.** (1997). Reverse genetics by chemical mutagenesis in *Caenorhabditis elegans*. *Nat. Genet.* **17**, 119-121.

**Johnson, K. G., Ghose, A., Epstein, E., Lincecum, J., O'Connor, M. B. and Van Vactor, D.** (2004). Axonal heparan sulfate proteoglycans regulate the distribution and efficiency of the repellent slit during midline axon guidance. *Curr. Biol.* **14**, 499-504.

**Kaech, S. M., Whitfield, C. W. and Kim, S. K.** (1998). The LIN-2/LIN-7/LIN-10 complex mediates basolateral membrane localization of the *C. elegans* EGF receptor LET-23 in vulval epithelial cells. *Cell* **94**, 761-771.

**Kinnunen, T., Huang, Z., Townsend, J., Gatdula, M. M., Brown, J. R., Esko, J. D. and Turnbull, J. E.** (2005). 2-O-sulfotransferase, *hst-2*, is essential for normal cell migration in *Caenorhabditis elegans*. *Proc. Natl. Acad. Sci. USA* **102**, 1507-1512.

**Kramer, K. L., Barnette, J. E. and Yost, H. J.** (2002). PKCgamma regulates syndecan-2 inside-out signaling during *Xenopus* left-right development. *Cell* **111**, 981-990.

**Lee, J. S. and Chien, C. B.** (2004). When sugars guide axons: insights from heparan sulphate proteoglycan mutants. *Nat. Rev. Genet.* **5**, 923-935.

**Lee, J. S., von der Hardt, S., Rusch, M. A., Stringer, S. E., Stickney, H. L., Talbot, W. S., Geisler, R., Nusslein-Volhard, C., Selleck, S. B., Chien, C. B. et al.** (2004). Axon Sorting in the Optic Tract Requires HSPG Synthesis by *ext2* (dackel) and *extl3* (boxer). *Neuron* **44**, 947-960.

**Leivonen, M., Lundin, J., Nordling, S., von Boguslawski, K. and Haglund, C.** (2004). Prognostic value of syndecan-1 expression in breast cancer. *Oncology* **67**, 11-18.

**Lindahl, U., Kusche-Gullberg, M. and Kjellen, L.** (1998). Regulated diversity of heparan sulfate. *J. Biol. Chem.* **273**, 24979-24982.

**Maduro, M. F., Gordon, M., Jacobs, R. and Pilgrim, D. B.** (2000). The

UNC-119 family of neural proteins is functionally conserved between humans, Drosophila and C. elegans. *J. Neurogenet*. **13**, 191-212.

**Merz, D. C., Alves, G., Kawano, T., Zheng, H. and Culotti, J. G.** (2003). UNC-52/perlecan affects gonadal leader cell migrations in C. elegans hermaphrodites through alterations in growth factor signaling. *Dev. Biol.* **256**, 173-186.

**Minniti, A. N., Labarca, M., Hurtado, C. and Brandan, E.** (2004). *Caenorhabditis elegans* syndecan (SDN-1) is required for normal egg laying and associates with the nervous system and the vulva. *J. Cell Sci.* **117**, 5179-5190.

**Morio, H., Honda, Y., Toyoda, H., Nakajima, M., Kurosawa, H. and Shirasawa, T.** (2003). EXT gene family member *rib-2* is essential for embryonic development and heparan sulfate biosynthesis in *Caenorhabditis elegans*. *Biochem. Biophys. Res. Commun.* **301**, 317-323.

**Perrimon, N. and Bernfield. M.** (2000). Specificities of heparan sulphate proteoglycans in developmental processes. *Nature* **404**, 725-728.

**Rogalski, T. M., Williams, B. D., Mullen, G. P. and Moerman, D. G.** (1993). Products of the *unc-52* gene in *Caenorhabditis elegans* are homologous to the core protein of the mammalian basement membrane heparan sulfate proteoglycan. *Genes Dev.* **7**, 1471-1484.

**Sasisekharan, R., Shriver, Z., Venkataraman, G. and Narayanasami, U.** (2002). Roles of heparan-sulphate glycosaminoglycans in cancer. *Nat. Rev. Cancer* **2**, 521-528.

**Sedita, J., Izvolsky, K. and Cardoso, W. V.** (2004). Differential expression of heparan sulfate 6-O-sulfotransferase isoforms in the mouse embryo suggests distinctive roles during organogenesis. *Dev. Dyn.* **231**, 782-794.

**Steigemann, P., Molitor, A., Fellert, S., Jackle, H. and Vorbruggen, G.** (2004). Heparan sulfate proteoglycan syndecan promotes axonal and myotube guidance by slit/robo signaling. *Curr. Biol.* **14**, 225-230.

**Topczewski, J., Sepich, D. S., Myers, D. C., Walker, C., Amores, A., Lele, Z., Hammerschmidt, M., Postlethwait, J. and Solnica-Krezel, L.** (2001). The zebrafish glypican knypek controls cell polarity during gastrulation movements of convergent extension. *Dev. Cell* **1**, 251-264.

**Zallen, J. A., Yi, B. A. and Bargmann, C. I.** (1998). The conserved immunoglobulin superfamily member SAX-3/Robo directs multiple aspects of axon guidance in *C. elegans*. *Cell* **92**, 217-227.

**Zallen, J. A., Kirch, S. A. and Bargmann, C. I.** (1999). Genes required for axon pathfinding and extension in the *C. elegans* nerve ring. *Development,* **126**, 3679-3692.